In-Situ Observation of Material Migration in Flip-Chip Solder Joints under Current Stressing

C.M. TSAI,[1] YI-SHAO LAI,[2] Y.L. LIN,[1] C.W. CHANG,[1] and C.R. KAO[3]

1.—Department of Chemical & Materials Engineering, National Central University, Jhongli City, Taiwan. 2.—Advanced Semiconductor Engineering, Inc., Kaohsiung City, Taiwan. 3.—Department of Materials Science & Engineering, National Taiwan University, Taipei, Taiwan; e-mail: kaocr@hotmail.com

This investigation studies how electron flow distribution and the vacancy concentration gradient affect the diffusion of solder atoms in a flip-chip solder joint under current stress. The migration of materials was traced by monitoring the positions of 21 Pb grains of the eutectic PbSn solder joint. Experimental results indicate that the displacements of the Pb grains were not uniform along the electron flow direction. Additionally, certain Pb grains exhibited lateral displacements. The nonuniform material migration is attributable to the combined effect of electromigration and the vacancy concentration gradient, which was caused by electromigration. By measuring the displacements of the Pb grains, we estimated that the DZ* value of Sn in eutectic SnPb solder was 5×10^{-10} cm^2/s.

Key words: Electromigration, flip-chip, PbSn solder

INTRODUCTION

Electromigration has long been known to cause failures in the interconnect lines of electronic devices, and recently electromigration has also become one of the major reliability concerns for flip-chip solder joints.[1–5] The electromigration problem in flip-chip joints is rather difficult to solve due to the complicated geometry of the solder joint. At the electron entrance to the solder joint, the path of electrons goes through a 90° turn and the cross-sectional area for electron flow increases by a factor of 100. This change in both electron flow direction and the cross-sectional area makes current crowding very pronounced.[6–8] Furthermore, near the electron entrance, where the local current density is high and the current crowding effect is strong, the local temperature is also high due to a Joule heating effect. The combined effect of high local current density, strong current crowding, and high local temperature causes the rate of material migration at this location (hereinafter, the current crowding region) to be the highest throughout the solder joint.

Our previous study on electromigration in eutectic SnPb solder joints at a mean current density of 3.1×10^4 A/cm^2 (at the contact window) indicated that the measured temperature near the current-crowding region increased from room temperature to 108°C by Joule heating.[9] Such a temperature is 83% of the eutectic PbSn temperature, and the lattice diffusion became the dominant mechanism of diffusion of Pb and Sn in the PbSn substrate. In the present investigation, the temperature and the current density were the same as those adopted in an earlier work.[9] Therefore, the dominant mechanism of atom migration is the vacancy diffusion through the lattice. Because both Pb and Sn diffuse in solders by the vacancy diffusion mechanism, a vacancy flux is established, in the opposite direction of the material migration flux.

This study examines how electron flow distribution and the vacancy concentration gradient affect the diffusion of solder atoms in a flip-chip solder joint under current stress. An in-situ observation is also made of the migration of materials caused by the diffusion of Pb and Sn of the flip-chip solder joints under current stress at room temperature. The migration of materials is traced by monitoring the positions of the easily observable Pb grains of the eutectic PbSn solder. In order to correlate the material migration with the electron current distribution, the electron current distribution was calculated using the finite-element approach.

EXPERIMENT

Figure 1a schematically depicts the samples used for in-situ electromigration testing. The solder was eutectic PbSn, and the solder joint had a normal diameter of 125 μm. The under-bump metallurgy

(Received March 1, 2006; accepted April 28, 2006)

(UBM) on the chip side was a layer of 8.5 μm-thick Cu with a dish-shaped rim. The metallization on the substrate side was in the form of a layer of 0.2-μm Au and a layer of 3-μm Ni, over the Cu conducting trace. The on-chip Cu lines had a width of 50 μm and a thickness of 5.5 μm. The opening diameter of the solder mask was 90 μm. Standard underfill was applied between the chip and the substrate.

The samples were cross sectioned to the center of the solder joints first to observe directly the surface of the joints during testing. During electromigration tests, the applied current was 1 A and the mean current density at the contact opening with a diameter of 90 μm was around 3.1×10^4 A/cm^2. This was the mean current density in the solder bump, not the current density in the current crowding region. The current stressing experiment was conducted at room temperature. Figure 1b presents the direction of electron flow. The electrons entered the joint from the upper-right corner, moved downward, and then left the joint through the conducting trace, pointing backward.

Changes in the surface microstructure were monitored with a scanning electron microscope (SEM). The phases were identified by energy dispersive x-ray spectroscopy. The surface temperature of the backside of the chip directly opposite the joints under current stress was measured by attaching a fine-gauge thermocouple. During current stressing, the temperature of the chip rose above the ambient temperature owing to Joule heating. The surface temperature of the backside of the chip rose with current-stressing time to a stable temperature of 108°C in about 10 min.

A finite-element simulation method was adopted because of the difficulty in measuring the local electric current density distribution in the solder joint. Since a constant electric current, I, is applied, the flow of electrons within metallic conductors constitutes a steady-state current that is consistent with the Laplace equation, $\nabla^2 V = 0$, where V is the electric potential, or voltage. The electrical resistances, R, of the metallic conductors are assumed to be independent of the applied voltage and the current, so Ohm's law, I = V/R, applies. Accordingly, the charge flow is analogous to the steady-state heat flow.[10,11]

According to Fig. 2, a two-dimensional finite element model, which involves the initial patterns of the Sn matrix and the Pb grains and the solder bump before current stressing, was constructed. The electrical resistivities of Cu, Sn, and Pb were 16.9 μΩmm, 110 μΩmm, and 206.5 μΩmm, respectively. The electron flow was assumed to have entered the solder bump from the top trace and to exit from the bottom trace, along the route that was supposed to be followed by the electrons in the actual experiment.

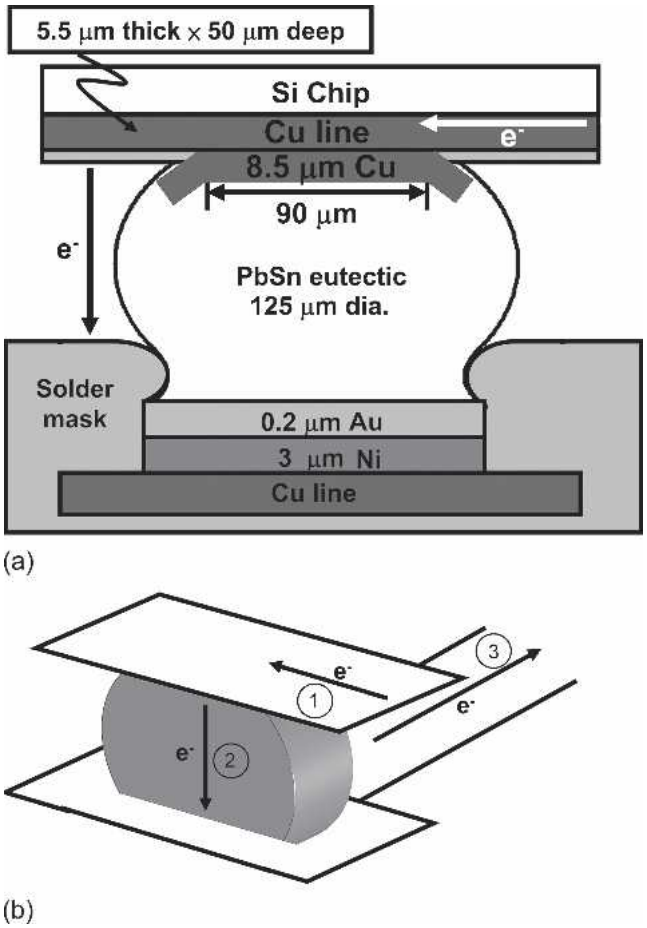

Fig. 1. (a) Schematic drawing showing the structure of the samples used for in-situ electromigration testing. (b) Direction of electron flow during current stressing. The electrons entered the joint from the upper-right corner ①, moved downward ②, and then left the joint through the conducting trace pointing backward ③.

RESULTS AND DISCUSSION

Sn Migration and Pb Grain Reorientation

Figure 3a–d displays SEM images of the cross-sectioned surface of the eutectic PbSn solder bump during current stressing of 0 min, 240 min, 400 min, and 1,000 min, respectively. The region presented here corresponds to the upper-right-hand corner of Fig. 2a. The bright phases in the joints were Pb-rich regions and the dark phases were Sn-rich regions. The scallop-type Cu_6Sn_5 compounds formed over the disk-shaped Cu UBM on the chip during the two reflows to assemble the joint. Additionally, many small particles are shown in Fig. 3c and d, between Cu and Cu_6Sn_5, extruding above the surface following current stressing. The analysis reveals that they were newly formed Cu_6Sn_5. In these micrographs, electrons entered the solder bump from the upper-right-hand corner and exited through the lower side.

As shown in Fig. 3a, the vertical distance from the top of the Pb grain in the lower-left corner to the bottom of the Cu_6Sn_5 grain in the upper-right corner was 14 μm before current stressing. The same distance in Fig. 3b decreased to 10 μm after 240 min of current stressing. As displayed in Fig. 3c and d, this corresponding distance then decreased to 8 μm and 6 μm after current stressing of 400 min and 1,000 min, respectively. The Cu_6Sn_5 was reasonably assumed to be stationary. Consequently, the only explanation for this decrease in distance was

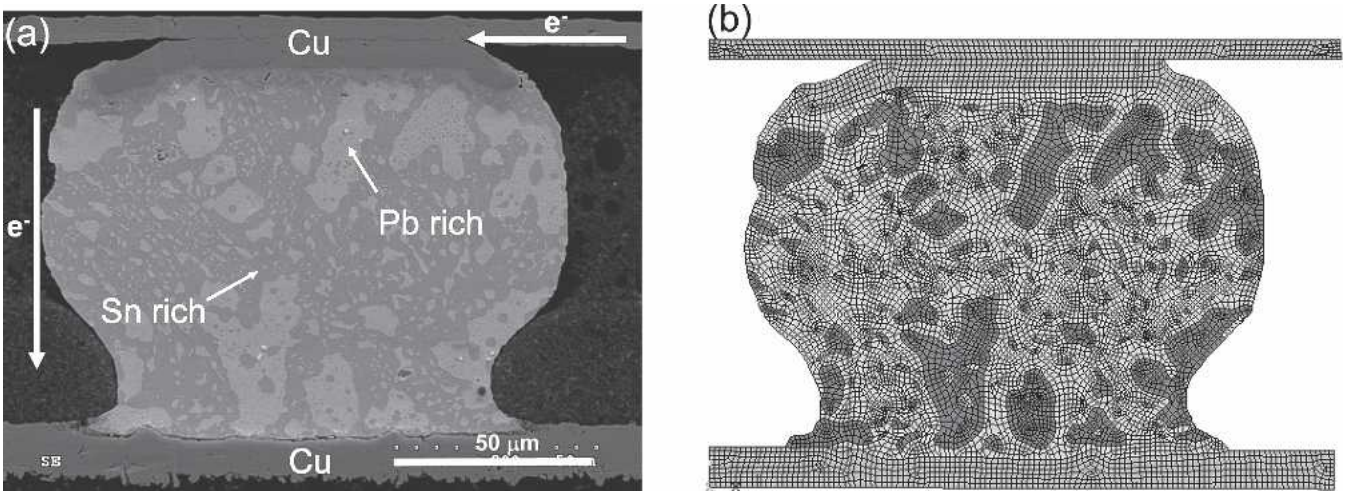

Fig. 2. (a) Microstructure of the solder joint before current stressing. (b) Two-dimensional finite element mesh, which involved initial patterns of Sn matrix and Pb grains shown in (a), used for the calculation.

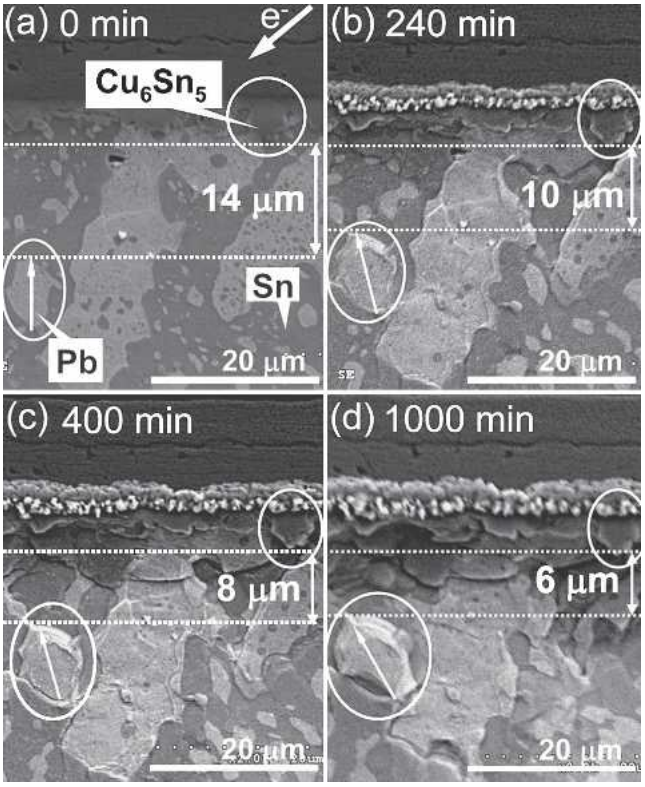

Fig. 3. SEM images of the cross-sectioned surface of the same joint during current stressing after (a) 0 min, (b) 240 min, (c) 400 min, and (d) 1,000 min current stressing. Electrons entered the solder bump from its upper-right-hand corner and exited through its lower side.

that the circled Pb grain had moved upward under current stressing. Since the electrons flowed downward from the chip side to the substrate side, in this particular case, the Pb grain was concluded to have moved in a direction opposite that of the electron flow. Since electromigration drives diffusion in the same direction, the upward movement of this Pb grain must be caused by the downward diffusion of the Sn atoms in the Sn-rich matrix. Briefly, Sn was concluded to be the dominant diffuser under current stress in this study. This result was reasonable because the solder temperature was about 108°C during current stressing and Sn had been reported to be the dominant diffusing species at temperatures below 120°C.[12]

The circled Pb grain in Fig. 3 not only moved upward, but also rotated counterclockwise during current stressing, as indicated by the arrow in Fig. 3a–d. High-resistance Sn grains have been reported to rotate to reorient themselves with respect to the neighboring low-resistance grains for in-current stressing experiments on the Sn stripe.[13] However, at this stage, whether the observed rotation of the Pb grain herein is caused in this way is unclear.

Analysis of Motion of Pb Grains

The positions of 21 Pb grains were monitored during current stressing, as shown in Fig. 4a, to analyze the diffusion behavior of Sn and Pb under current stressing. The unreacted Cu conducting trace at the lower left-hand corner was taken as the fixed frame of reference. The positions (x and y coordinates) of these 21 Pb grains during current stressing were recorded and plotted in Fig. 4b. All of these 21 Pb grains moved upward with current stress, revealing that Sn was pushed downward by electromigration throughout the entire joint.

In Fig. 4c, the solder joints were divided into three regions according to the distance migrated in the vertical direction after 1,000 min of stressing. The displacement was 2–3 μm in the vertical direction in region A, 5–6 μm in region B, and 8–10 μm in region C. In the central region C, much of the material had migrated, indicating that most of the electrons passed through C. In region B, the migration was less substantial, and in region A, the migration was the smallest, indicating that fewer electrons passed through regions A and B than passed through region C. In short, the experimental results demonstrated that the distribution of the current flow was very inhomogeneous in the solder bump.

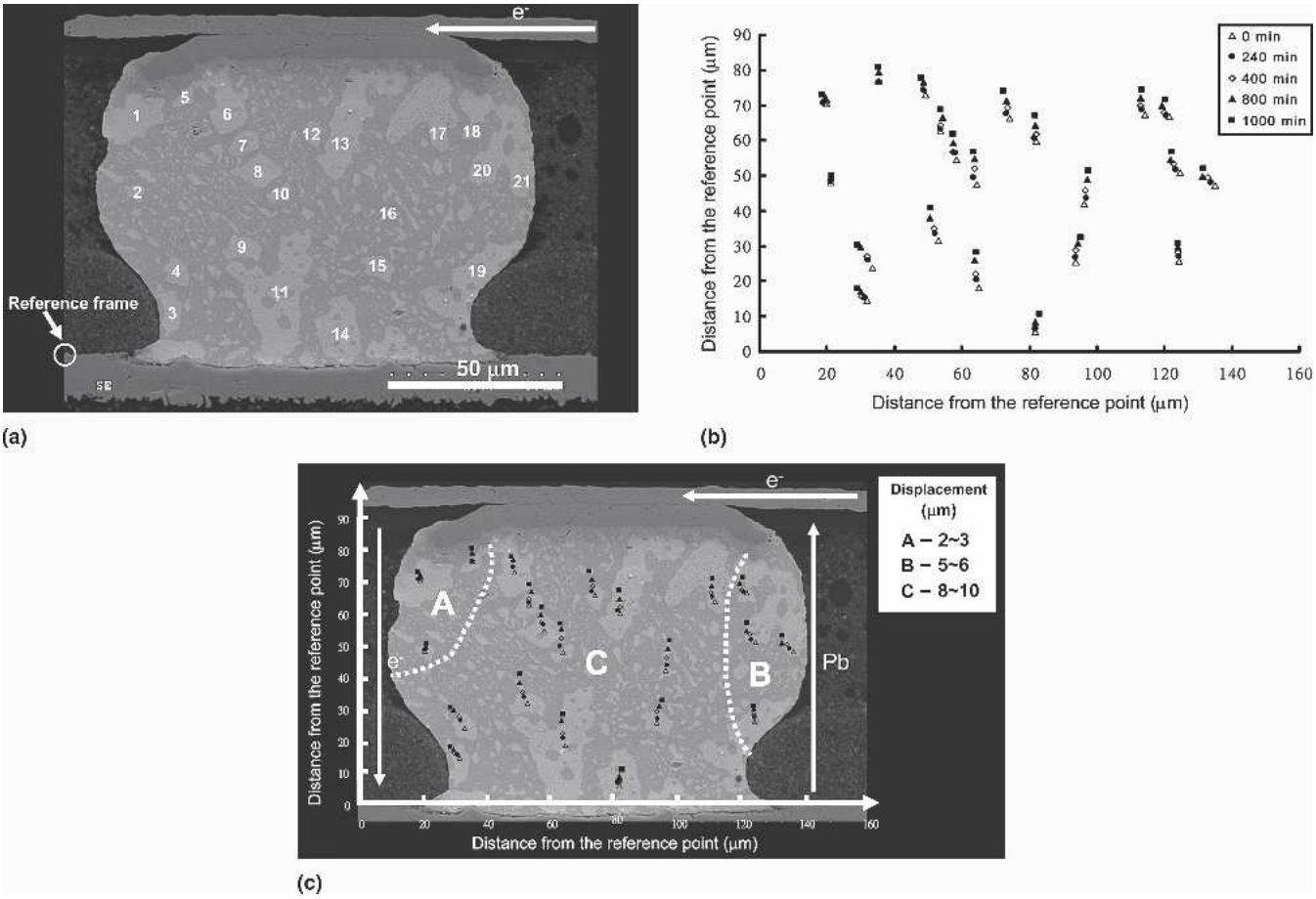

Fig. 4. (a) Original positions of the 21 Pb grains monitored during current stressing. The unreacted Cu conducting trace at the lower-left corner was used as the fixed frame of reference. (b) Coordinates of the 21 Pb grains recorded after 0 min, 240 min, 400 min, 800 min, and 1,000 min of current stressing. (c) Three regions, A–C, according to the vertical migration distance after 1,000 min of stressing.

The calculated electron current distribution, which is shown in Fig. 5, is now considered. The figure indicates that current crowding occurs around the corner where the electric current flows from the Cu trace to the solder bump. Additionally, Pb grains disturbed the flow field because the Pb phase had a resistivity double that of Sn and the electrons tended to avoid entering the Pb phase. The current density distribution displayed here matches nicely the migration distances presented in Fig. 4. Fewer electrons passed through regions A and B, and less material migration occurred. The current density was highest in region C, in which the amount of material that migrated was also the highest.

Figure 4b also shows that the migration of the Pb grains, especially those located in the upper-right-hand corner—grains 18, 20, and 21—was not limited to the vertical direction. These grains also migrated laterally. The lateral migration suggests a Sn flux in this direction. Figure 6 displays microstructural evidence. Figure 6a and b shows magnified images of the upper right-hand corner of the joint before and after stressing for 400 min, respectively. The Sn-rich region in Fig. 6a disappeared after 400 min of current stressing, as shown in Fig. 6b. Since relatively few electrons passed through this region, electromigration was not likely to be the direct mechanism of the disappearance of the Sn-rich region in Fig. 6. We suggest that the Sn-rich region disappeared due to current crowding, which worked in the following sequence. First, in

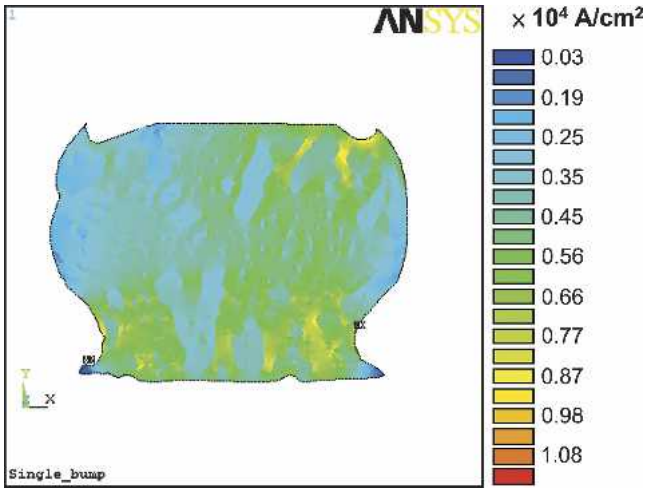

Fig. 5. Calculated electron current distribution. The mesh for this calculation is shown in Fig. 2b.

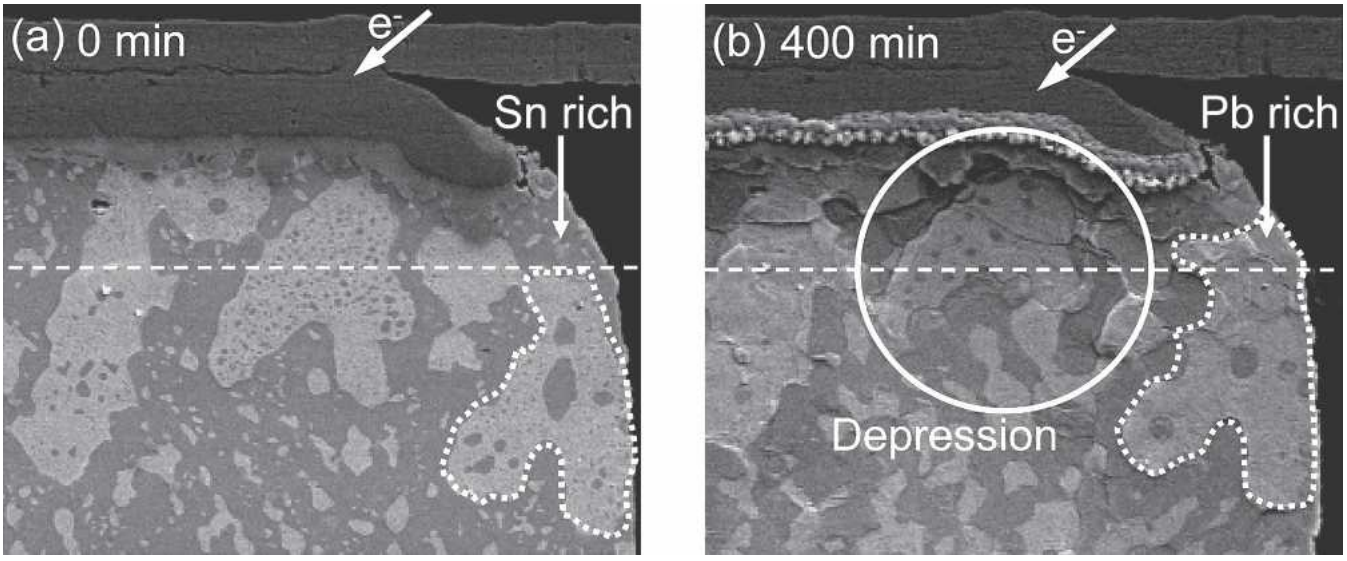

Fig. 6. Zoom-in pictures showing the upper-right corner of the joint (a) before stressing and (b) after stressing for 400 min.

the region of high current density, the Sn atoms were driven downward by electromigration. As the Sn atoms diffused away, a vacancy flux diffused in the opposite direction, reaching the region near the interface between Cu and the solder. Therefore, the concentration of vacancies increased. In order to decrease the vacancy concentration here, the vacancy diffused to the right, and consequently an opposite Sn flux diffused to the left. This Sn diffusion flux to the left was responsible for the disappearance of the Sn-rich region.

The current density simulation yields information on the electron flow direction and the density at every location. Figure 7a shows the information at selected locations. Based on the assumption that the migration of Pb grains presented in Fig. 4b can be adopted to approximate the relative magnitude and the reversal direction of the Sn flux, Fig. 7b plots the Sn flux at selected locations. Figure 7c plots the data in Fig. 7a and b together. This figure shows that for the majority of these selected locations, the directions of electron charge flow match the initial movements of Pb grains, which may provide supporting evidence of the correlation between these two phenomena. Notably, the experimental observations were made over a period during which the vacancy flux diverged, inducing additional diffusion (current crowding effect), but the numerical results refer only to the directions of initial flow of electron charges, because the numerical model considered only the solder bump at its initial stage. Furthermore, the numerical model also cannot represent the diffusion of complex atoms.

According to the above discussion, electromigration induced a primary Sn flux and the vacancy gradient induced a secondary Sn flux. The primary Sn flux directly induced by electromigration was directed downward, and the secondary Sn flux induced by the vacancy concentration gradient was directed from right to left. Since the direction of the electron charge flow matched that of the Sn atoms nicely in region C, the dominant diffusion mechanism in region C was inferred to be by electromigration only. Therefore, the medium Pb grain displacement in region C, 9 μm, is used to calculate the DZ*. Based on the assumption that the Sn matrix had the same displacements but in the opposite direction as the Pb grains under stressing, the drift velocity ν of Sn is estimated to be 9 μm/1,000 min. The mean atom drift velocity ν caused by the electron current is given by the following equation:

$$\nu = \frac{DeZ^*}{kT}\rho j \tag{1}$$

where D is the diffusion coefficient, e is the electron charge, Z* is the effective charge number of the Sn atom, ρ is the metal resistivity, j is the electron current density, k is Boltzmann's constant, and T is the absolute temperature. Here, the average current density of 3.1×10^4 A/cm^2 is used for j, and T is 381 K. The ρ value is 32 μΩcm at 100°C.[14] From Eq. 1, DZ* was calculated to be 5×10^{-10} cm^2/s.

CONCLUSIONS

The effect of electromigration and current crowding on solder bump was observed in situ. In the central region of the joint, the Sn flux was driven mainly by direct electromigration, and produced a primary Sn flux in the same direction as the electron flow. Furthermore, a secondary Sn flux was near the current crowding region. This flux was generated by the vacancy concentration gradient and was toward the current crowding region. The vacancy concentration gradient was induced by direct electromigration. The displacements of the Pb grains were measured, and the DZ* value of Sn in eutectic SnPb solder was estimated to be 5×10^{-10} cm^2/s.

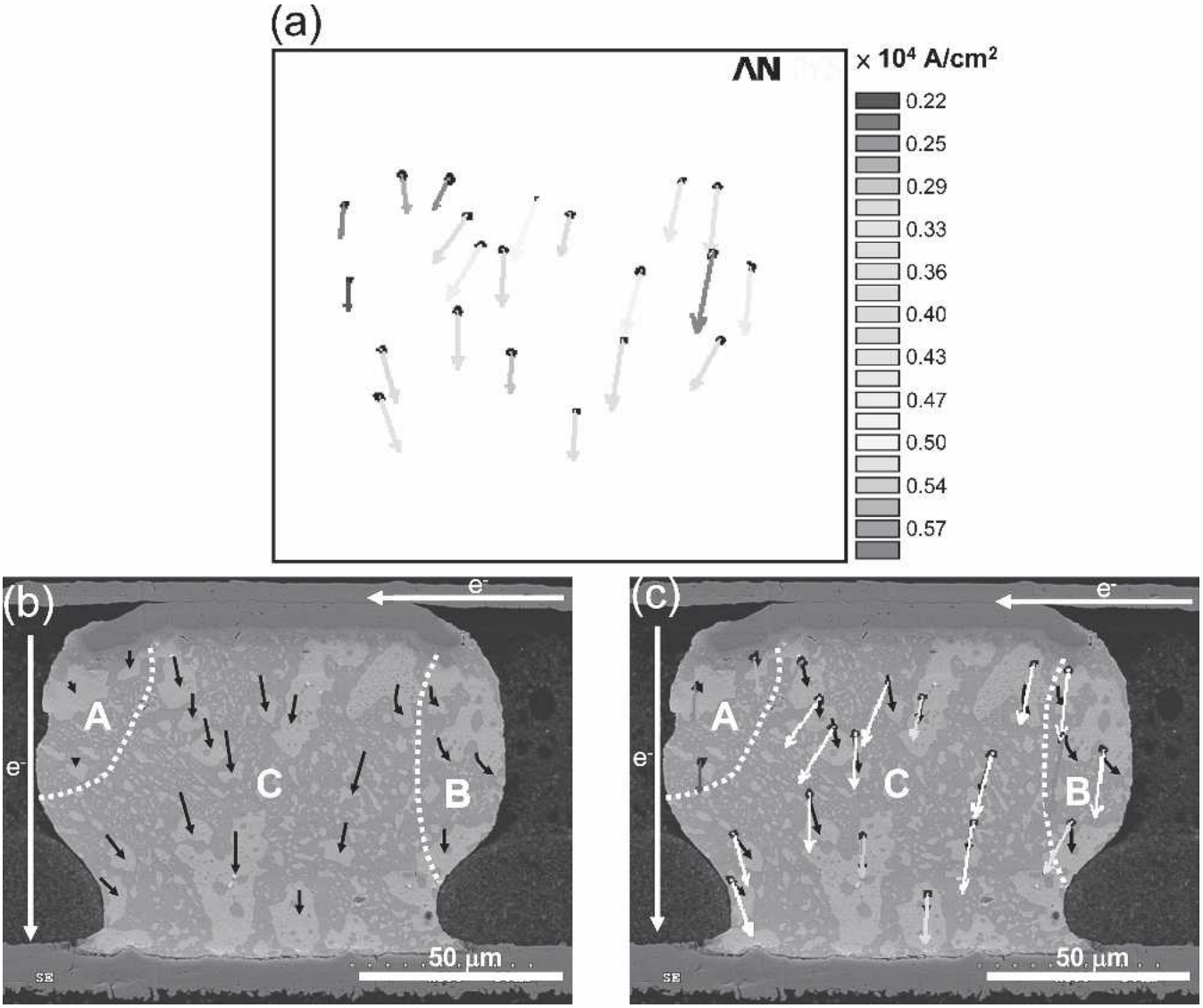

Fig. 7. (a) Electron flow direction and density at selected locations from the numerical simulation. (b) Estimated Sn flux by assuming that the Pb grain migration shown in Fig. 4b can be used to approximate the relative magnitude and the reversed direction of the Sn flux. (c) Information in (a) and (b) plotted in the same graph for comparison.

ACKNOWLEDGEMENTS

The authors thank the National Science Council of the Republic of China, Taiwan, for financially supporting this research under Contract Nos. NSC-94-2216-E-008-001 and NSC-94-2214-E-008-005.

REFERENCES

1. E.C.C. Yeh, W.J. Choi, K.N. Tu, P. Elenius, and H. Balkan, *Appl. Phys. Lett.* 80, 580 (2002).
2. Y.C. Hu, Y.H. Lin, C.R. Kao, and K.N. Tu, *J. Mater. Res.* 18, 2544 (2003).
3. Y.H. Lin, Y.C. Hu, C.M. Tsai, C.R. Kao, and K.N. Tu, *Acta Mater.* 53, 2029 (2005).
4. A.T. Wu, K.N. Tu, J.R. Lloyd, N. Tamura, B.C. Valek, and C.R. Kao, *Appl. Phys. Lett.* 85, 2490 (2004).
5. K.N. Tu, *J. Appl. Phys.* 94, 5451 (2003).
6. Y.L. Lin, C.W. Chang, C.M. Tsai, C.W. Lee, and C.R. Kao, *J. Electron. Mater.* 35, 1010 (2006).
7. Y.H. Lin, C.M. Tsai, Y.C. Hu, Y.L. Lin, and C.R. Kao, *J. Electron. Mater.* 34, 27 (2005).
8. Y.H. Lin, C.M. Tsai, Y.C. Hu, Y.L. Lin, J.Y. Tsai, and C.R. Kao, *Mater. Sci. Forum* 475–479, 2655 (2005).
9. C.M. Tsai, Y.L. Lin, J.Y. Tsai, and C.R. Kao, *J. Electron. Mater.* 35, 1005 (2006).
10. T.-Y.T. Lee, T.Y. Lee, and K.N. Tu, *IEEE Trans. Compon. Packaging Technol.* 27, 472 (2004).
11. D. Halliday and R. Resnick, *Fundamentals of Physics* (New York: John Wiley & Sons, 1974), pp. 512–514.
12. D. Gupta, K. Vieregge, and W. Gust, *Acta Mater.* 47, 5 (1999).
13. A.T. Wu, A.M. Gusak, K.N. Tu, and C.R. Kao, *Appl. Phys. Lett.* 86, 241902 (2005).
14. R.J. Klein Wassink, *Soldering in Electronics* (New York: Electrochemical Society, 1989), pp. 166–167.